UNIVERSITY OF CALIFORNIA,
IRVINE

Optimization and Testing of the Design of a Neural Probe Device

THESIS

submitted in partial satisfaction of the requirements
for the degree of

MASTER OF SCIENCE

in Biomedical Engineering

by

Christopher Tu

Thesis Committee:
Professor William C. Tang, Chair
Associate Professor Zoran Nenadic
Assistant Professor Beth Lopour

2014

DEDICATION

Thanks to my mother

TABLE OF CONTENTS

LIST OF FIGURES

ACKNOWLEDGMENTS

I would like to thank Dr. Dhonam Pemba for his guidance, assistance, and motivational words during the course of the project. Without his amazing work on designing and building the neural probes, I would not have been able to complete this thesis. I would also like to thank fellow student Tina Zhu, whose electronics skills, particularly in soldering, were a key part of the thesis as well. Professors Zoran Nenadic and Beth Lopour were kind enough to be on the thesis committee and provide me with valuable feedback. Finally, I would like to show my appreciation to Professor William Tang, who showed me kindness and generosity in allowing me to work on this project.

ABSTRACT OF THE THESIS

Optimization and Testing of the Design of a Neural Probe Device

By

Christopher Tu

Master of Science in Biomedical Engineering

University of California, Irvine, 2014

Professor William C. Tang, Chair

A model of an SU-8 neural probe electrode containing both an embedded fluid channel for fluid delivery and nerve stimulation and recording abilities was created using COMSOL software. A mechanical model of the neural probe electrode was simulated using COMSOL while varying several design parameters in order to better optimize the physical design of the electrode. It was found that the thickness of the neural probe should be from 0.35 mm to 0.5 mm, as the effects of increasing thickness beyond 0.5 mm on maximum stress were not very significant. Additionally, the ideal length of the neural probe was found to be between 4.5 and 5.5 mm to minimize stresses in the neural probe. The ability of the neural probe device to record electrical signals was tested in biological tissue, specifically in frog nerves, using LabVIEW software and myDAQ hardware as well as a device designed for electrophysiology experiments called a "SpikerBox." Compound action potential signals from exposed frog nerves were successfully recorded using the neural probes and the SpikerBox device.

Introduction

An estimated 185,000 persons undergo an amputation of an upper or lower limb each year in the United States, and about 1.7 million people currently live with limb loss as of 2005 (Ziegler-Graham). This number is projected to double by the year 2050 due to the aging of the population and the increase in the number of people living with conditions such as diabetes that could lead to amputation of a limb. The use of prosthetics can improve quality of life for patients who have lost a limb by restoring the function of the missing limb. A significant percentage (58.5%) of trauma-related amputations involved upper limbs, suggesting that upper limb prosthetic devices would be beneficial to many patients.

The purpose of a neural probe device is to create an interface to communicate with nerves directly and to provide a method of controlling prosthetic devices. Neural probe electrodes implanted in peripheral nerves can be used for both stimulation of motor fibers and recording from sensory nerve fibers. For upper limb prosthetics, the main target of the neural probe is the brachial plexus, which is a network of nerve fibers that innervates the upper limb. Control of a prosthetic limb can be made more difficult depending on where the limb was removed. For example, removal of the limb at the shoulder requires many more functions to be controlled, including the shoulder joint, elbow and wrist. However, the brachial plexus is large enough that prosthetic control with a neural probe device can still be possible even if the upper limb is amputated at the shoulder.

Intrafascicular electrodes that are designed for implantation into a nerve fascicle (a bundle of nerve fibers) can potentially allow for selective stimulation or recording of peripheral nerves. Selective stimulation of individual motor units or small groups of axons has been demonstrated experimentally with implanted arrays (Grill et al.). Intrafascicular electrodes are

also electrically shielded due to the presence of surrounding nerve tissue, further improving stimulation and recording capability (Branner). It is advantageous to arrange the electrodes in an array, as it is possible for some of the electrodes to break while being implanted or to miss the nerve fascicles completely (Branner). Selectively stimulating and recording from individual nerve fascicles can lead to finer control of a prosthetic device.

One major issue with chronically implanted electrodes is that their functionality decreases the longer they are implanted, due to damage to the nerve in which they are implanted and the immunological response by the body. Since intrafascicular electrodes are designed to penetrate the nerve, they can compromise the connective tissue protecting the nerve, leading to edema, fibrosis and the eventual loss of nerve fibers. A possible solution to this problem is the injection of drugs or growth factors directly into the nerve. Growth factors such as VGF or neurotrophins can prevent or reduce neural degeneration, which in turn allows the neural probe to continue functioning. By integrating fluid channels within the neural electrode, it becomes possible to deliver drugs or growth factors directly to the nerve and thereby increasing the longevity of both the electrode and the nerve. In this way, long-term control of a prosthetic device through the use of the electrodes may become possible.

One area of concern for the neural probe electrode is that it may snap or break during implantation or if it experiences large forces while it is implanted. Computer simulation may be useful in determining how to best optimize the design of the neural probe in order to minimize this occurrence.

Background

Brachial plexus and nerve structure

The brachial plexus is a network of nerve fibers that is responsible for sensory and motor innervation of the upper limb; it is built up from the spinal nerves at five levels from C5 to T1. Injury to the brachial plexus can result in loss of sensory and motor function.

Nerves in the peripheral nervous system are organized into bundles that contain several types of connective tissue with different mechanical properties. The endoneurium is a layer of tissue that encloses a nerve fiber and the layer of myelin around it. A bundle of nerve fibers forms a fascicle, which is surrounded by the perineurium. The perineurium consists of layers of collagen and perineurial cells, which maintains homeostasis of endoneurial fluid surrounding the nerve fibers. The outermost layer is the epineurium, which groups together several fascicles and a blood supply (Stewart). Peripheral nerves vary in size, with some nerves, such as the sciatic nerve, being large enough to be visible with the naked eye; other nerves can require significant magnification to be seen with any detail.

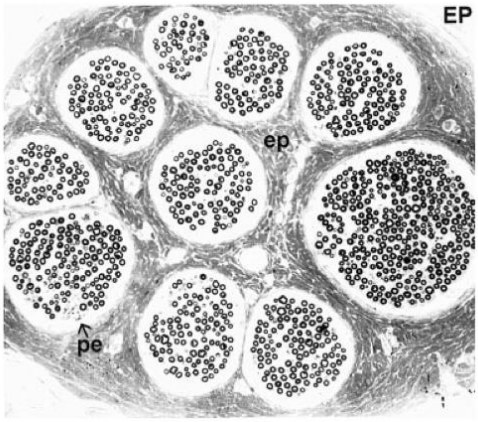

Figure 1. A cross section of a mammalian peripheral nerve with 10 fascicles. Perineurium (pe) encloses nerve fibers to form fascicles. The dark tissue in between contains the endoneurium (ep) and unmyelinated nerve fibers. All of the fascicles are surrounded by a layer of epineurium (EP) The magnification factor used was 180x. (Stewart)

Obstacles to neural probe function

There are several obstacles that can affect the proper functioning of an implanted neural probe. If the neural probe does not have good biocompatibility with the surrounding tissue, the body's immune response can affect how well the interface works over time. It is also important that the mechanical properties of the probe are similar to those of the tissue in order to minimize unwanted tissue damage; for example, the use of SU-8 rather than silicon to form the body of the electrode may be advantageous due to the lower stiffness of SU-8. In contrast, a probe formed out of silicon, which has a much higher stiffness than nerve tissue, may cause significantly more damage when implanted as well as provoking a stronger immune response from the body. Motion of an implanted silicon probe can cause tissue damage while also reducing accuracy or introducing noise into the measured signal; in contrast, a probe made of SU-8 is more flexible and can bend with an applied force, preventing damage from occurring (Tijero). Damage to peripheral nerves can cause loss of function, so it is desirable to minimize the damage caused during implantation.

Electrode shape is a possible factor that can influence the level of fibrotic encapsulation. For example, electrodes with a large cross-sectional area and sharp edges cause a more severe tissue reaction when implanted in the central nervous system, which suggests that the peripheral nervous system would be affected in the same way (Grill et al). Another way that fibrosis can be reduced is through the design of the electrode surface; for example, the surface can be coated with anti-inflammatory compounds that are gradually released into surrounding tissue.

Another challenge that neural probe interfaces have to overcome is the low amplitude of nerve signals and many sources of noise from surrounding tissues. For example, electromyogram

(EMG) signals from activated muscles may cover up signals from peripheral nerves, which would inhibit signal recording from those nerves (Grill et al).

Frog sciatic nerve

The frog sciatic nerve consists of a large number of nerve fibers of varying sizes and properties, such as responsiveness to stimulus and action potential conduction velocity. An action potential can be generated in a section of nerve when its membrane becomes slightly depolarized to a threshold voltage, causing voltage-gated sodium channels to open. When the sciatic nerve is stimulated using an applied voltage, it produces a response that is the summation of the responses of its component nerve fibers. This response can be observed and recorded as a compound action potential (CAP). The magnitude of the compound action potential can be altered by varying the intensity or duration of an applied stimulus, which affects the number and type of nerve fibers that are activated.

Procedures

Current probe design overview

The current neural probe design contains a square head that is 2 mm (2000 μm) on each side and contains gold pads for interfacing with external devices, as well as the inlet channel at the top of the probe for fluid delivery. Extending from the base of the head is a 5 mm long needle that is used for penetrating the peripheral nerve tissue. The needle also contains gold wires and pads for interfacing with nerve tissue, as well as the outlet channels for fluid delivery. The neural probe body is composed of an SU-8 layer with a thickness of 250 μm. The fluid channel is placed at a depth of 35 μm from the top face of the neural probe body.

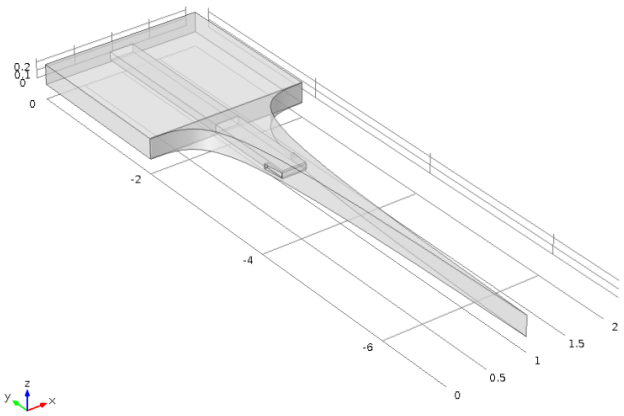

Figure 2. 3D model of the neural probe electrode, generated in COMSOL.

Computer simulation of the mechanical properties of the neural probe will be useful for determining the optimal dimensions of both the probe and the embedded fluid channel used for drug delivery. The shape of the electrode must be designed in such a way that it is strong enough to penetrate the nerve without bending or breaking, while also being thin enough to avoid causing too much unwanted damage to the nerve. Additionally, the cross-sectional area and the

number of sharp features should be minimized to reduce the amount of fibrous encapsulation around the electrode.

A previous study has shown that the required force for piercing a porcine peripheral nerve with a needle is in the range of 0.3 to 25 mN, depending on the velocity with which the needle was inserted, which ranged from 1 to 2000 mm/min (Sergi). Another study of insertion force of a tungsten needle into peripheral nerve found that the needle had to be able to sustain an axial load of at least 2 mN without breaking or causing other damage to the electrode (Jensen). Given that SU-8 is not nearly as rigid as tungsten, silicon or other metallic materials, some revision of the current design, such as shortening the needle length or increasing the thickness of the electrode, may be necessary to ensure that the needle is able to penetrate the nerve without breaking.

In vivo testing of SU-8 microneedles has found that they can be viable for implantation in the brain (Fernandez). However, there are differences in the composition of brain tissue and peripheral nerve tissue that can make implantation into peripheral nerves more difficult. One of the primary components found in peripheral nerve is collagen, which provides compressive and tensile strength that protects axons during motion and other types of loading (Nicholson). The presence of collagen in peripheral nerves means that more force may be needed to successfully insert the needle compared to brain tissue.

I. COMSOL modeling

Modeling of the neural probe's mechanical properties was performed using COMSOL Multiphysics version 4.2 software. A 3D model of the electrode was generated using COMSOL, and the parametric sweep feature was used during simulation to determine results for different lengths of the electrode's needle, in order to assess whether or not altering the length would have

any effect on the results. The parametric sweep feature was also used to compare different thicknesses of the neural probe body, as well as different depths at which the fluid channel was placed. The experimental needle lengths were 3.5, 4.5, 5.5 and 6.0 mm. Experimental neural probe thicknesses were 0.25, 0.35, 0.45 and 0.50 mm. The experimental fluid channel placements were 35, 45, 55, 65, 75 and 85 μm from the top surface of the probe. SU-8 was chosen as the material for the 3D model, with an elastic modulus E = 4.02 GPa, a Poisson's ratio of 0.22, and a density of 1.2 g/cm^3. The simulations involved applying simulated loads from 10 to 50 mN to the top and the side of the neural probe's needle. After sweeping through each possible combination of the three variables (needle length, fluid channel depth, and neural probe thickness), the plots generated from COMSOL were examined to determine the maximum value of stress in the neural probe. This data was then plotted using Excel in order to determine the effects of each parameter on the stress value.

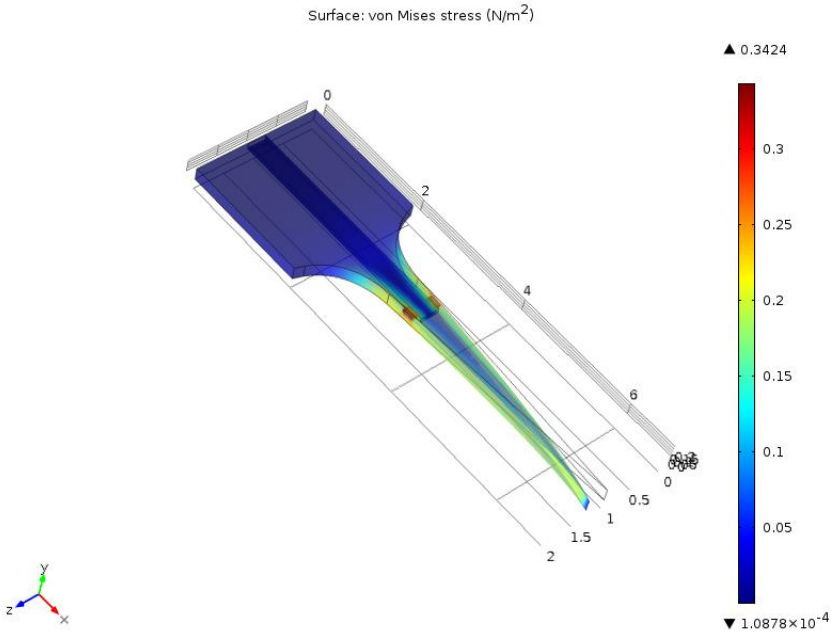

Figure 3. An example output image from simulations using COMSOL.

The purpose of varying the needle length, probe thickness, and fluid channel depth during simulation was to determine whether or not modifying these parameters will cause a significant change in the maximum stress felt by the probe under an applied load. The simulation results may also be useful in determining optimal values for these parameters that would minimize the stress on the probe under load.

II. Electrical testing of the neural probe

In order to verify the electrical conductivity of the neural probe, attempts were made to see if the device could both transmit and receive electrical signals. Initially, electrical conductivity tests were performed with the neural probes attached to wires using a silver epoxy material. These tests were conducted with two of the neural probe devices; one probe was used for sending the signal, while the other was used to receive the signal. The tests were conducted at approximately room temperature. The probe that was used for signal transmission was connected to a function generator that created a sinusoid shaped signal, while the probe being used for receiving was connected to an oscilloscope to read the signal. Both of the probes were inserted into a beaker of 0.9% saline solution which was able to conduct electrical current. After inserting the probes and turning on the function generator and oscilloscope, the oscilloscope screen showed a sinusoid signal matching the signal that was created using the function generator. The results of the initial test demonstrated that the probes were conductive and able to send and receive a signal from a function generator when placed in a conductive solution.

In order to perform more tests on the electrical conductivity of the devices, particularly when used in actual biological tissue, LabVIEW software and the National Instruments myDAQ data acquisition device was chosen to create a simple signal generation and acquisition program.

An off-the-shelf device called the SpikerBox, which was designed specifically for performing simple neuroscience experiments, was also used to test the neural probe devices.

1. Initial electrical test using saline solution

First, in order to verify the functionality of the LabVIEW program and the myDAQ device, the previous tests using 0.9% saline solution and the physical oscilloscope and function generator were repeated using a LabVIEW program. This was possible due to LabVIEW's ability to simulate hardware devices such as the function generator and oscilloscope. The LabVIEW virtual instrument program for this section was very simple and involved the use of the DAQ assistant, which allowed for easy implementation. The block diagram for the program was very simple and consisted of two loops. The first loop sent a simulated sine wave or other signal to the analog output wire on the myDAQ, while also displaying the generated signal on a waveform chart in the program's front panel. The second loop read a signal from the analog input wire and displays the signal on another waveform chart. To perform the test, the analog output and input wires, which were both attached to the neural probes, were inserted into a small container of 0.9% saline solution at room temperature. A breadboard was used in order to make access to the analog input and output easier, as the wires used for the test were fairly short in length.

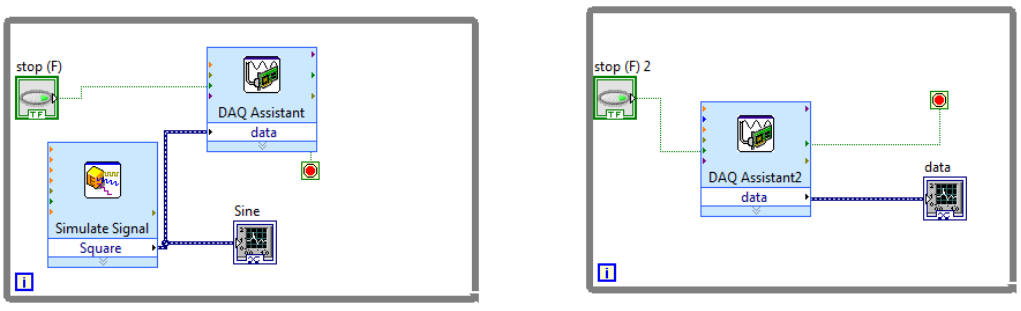

Figure 4. The block diagram of the LabVIEW program that was used for initial testing.

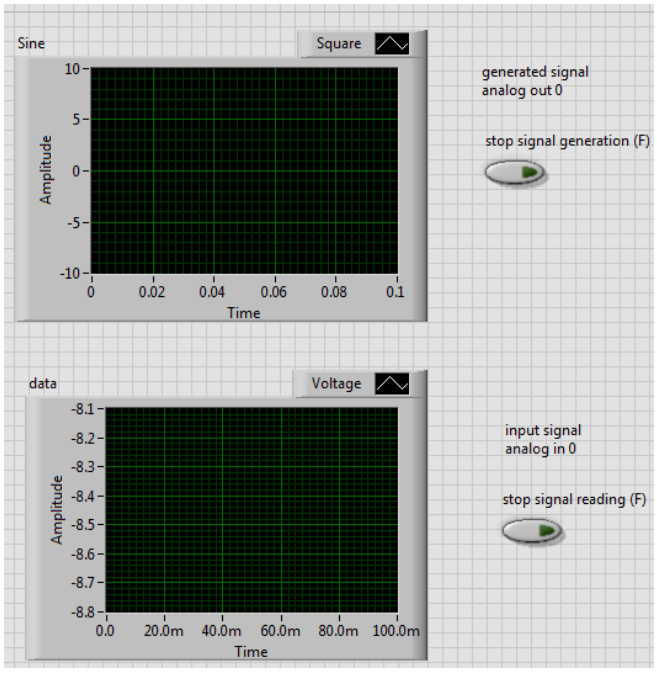

Figure 5. The front panel of the LabVIEW program.

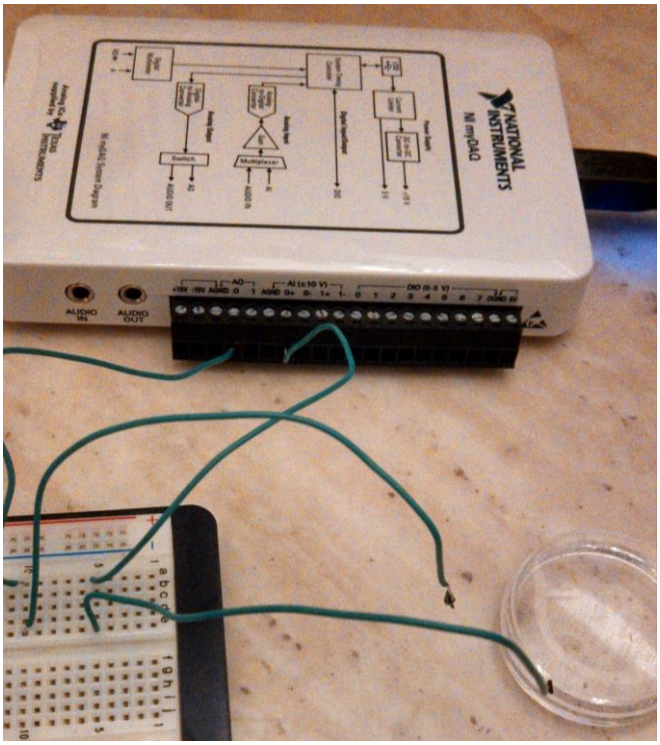

Figure 6. The myDAQ, wires attached to neural probes, and petri dish containing 0.9% saline solution.

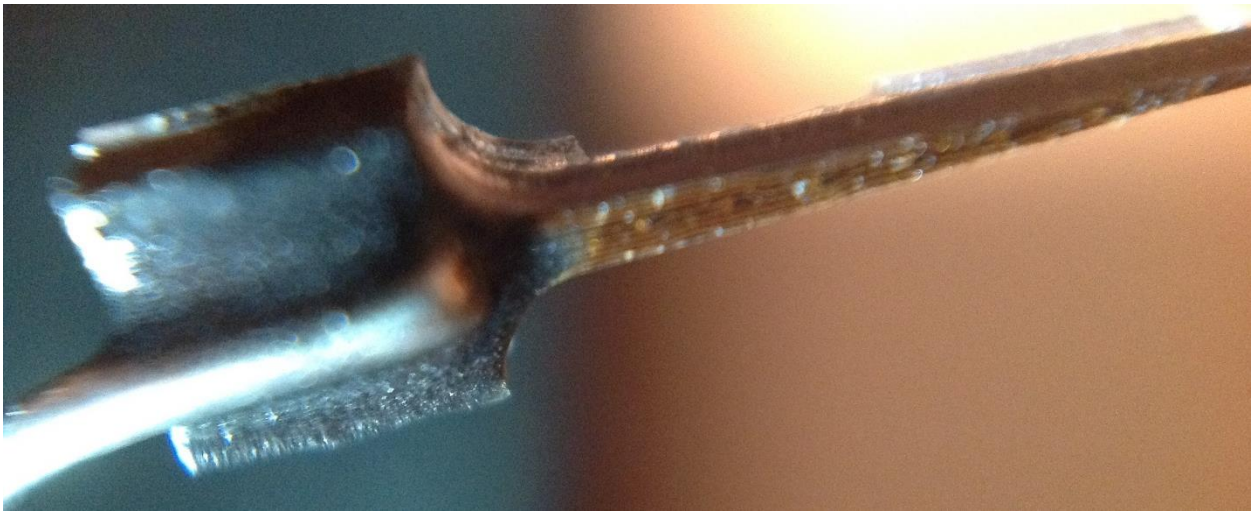

Figure 7. A closer view of the neural probe attached to a wire with a conductive adhesive.

After verifying that the LabVIEW program was functional, the next step was to see if the neural probes could function in biological tissue, such as muscle or nerve tissue. The same program from the initial LabVIEW test was used. The neural probes were placed in contact with an exposed nerve of a sacrificed frog approximately 2 to 3 cm apart, and the output of the program was examined to see what kinds of signals could be recorded.

Figure 8. Neural probes placed in contact with an exposed nerve of the frog.

2. Frog sciatic nerve test

Another approach to recording signals from the frog nerves was also attempted. One common method of learning about muscles and nerves in physiology classes is through experiments related to a frog's sciatic nerve, since it is relatively large and easy to access, especially compared to other experimental animals. Using the frog sciatic nerve was suggested for testing the neural probe devices because its use in electrophysiology experiments was well-established and documented.

The same LabVIEW program used previously was used for the purpose of generating stimulus signals and recording any output signals from the nerve. Additionally, a different experimental setup involving more electrodes was needed compared to the initial tests. Voltage signals can be measured either relative to a ground, which can be considered to be at 0 volts, or between two points, which is referred to as a differential voltage measurement. One of the electrodes would provide the reference, while the other would be used to record voltages relative to that reference.

For the sciatic nerve experiments, removing the nerve from the leg may be preferable. Compound action potentials recorded from the isolated sciatic nerve can be expected to be in the range of 1 to 10 mV. In contrast, if the nerve is still situated within the leg, signals acquired from the surface of the leg would be on the order of 10 μV, which would be very difficult to acquire without a significant amplification of 10^5 (Olansen et al).The nerve is positioned next to the femoral artery in the thigh of the frog. Frog dissection was performed in accordance with the "Electroneurology" lab manual from Rice University. Briefly, muscles in the thigh of the frog were cut and bluntly dissected and separated in order to expose the artery and nerve. The ends of the nerve length to be removed were tied with thread, and the nerve was cut beyond where the thread was tied. One disadvantage of removing the nerve from the body of the frog is that it

quickly dries out and becomes nonviable unless it is frequently coated with fluid. When the nerve is still situated in the body, it is surrounded by tissue that keeps it moist and can remain viable for a longer period of time, at the cost of having more noise interfering with the signal.

Figure 9. The thigh muscle of the frog cut and separated to expose the femoral artery and sciatic nerve.

The myDAQ's analog inputs contained a 16-bit ADC that has a range of ±10 V, which should be sufficient to detect nerve signals in the mV range. Based on the wiring diagram from the myDAQ manual, one neural probe was connected to the myDAQ's positive analog input, and another to the negative analog input. The negative input was also connected to the ground port on the myDAQ. This was necessary to provide the proper inputs into the instrumentation amplifier of the myDAQ and to set one of the inputs as a reference, since voltage needs to be measured relative to a baseline value.

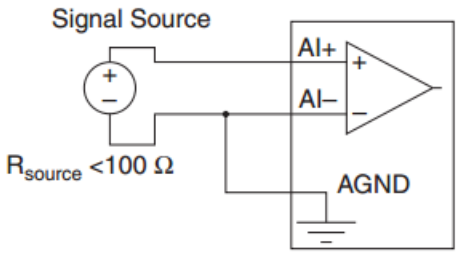

Figure 10. MyDAQ wiring diagram.

Two approaches to recording were tried. In the first approach, a section of sciatic nerve approximately 2 to 3 cm in length that was removed from one leg of the frog was laid over the two neural probes, and stimulation was provided using the LabVIEW program. The nerve was

exposed to air for 30 seconds to 1 minute before any recording attempts were made, and was kept moist by the application of 0.9% saline solution. In the second approach, neural probes were inserted into the exposed nerve in the other frog leg, where stimulation was provided by physically manipulating the frog muscles. All of the attempts to record signals were performed at room temperature.

3. Experiment with frog nerves using the SpikerBox

An inexpensive off-the-shelf device called the SpikerBox (University of Michigan) that was designed specifically for simple neuroscience experiments was also used in an attempt to record frog nerve signals. The device consists of a small circuit board, powered by a 9-volt battery, containing various components that allow electrical impulses from nerves to be recorded through the microphone port on any computer. The device was purchased as a kit and assembled and soldered according to the provided instructions. A schematic of the SpikerBox device can be seen on the website for the product (www.backyardbrains.com). To briefly describe the function of the device, the electrodes that interface to nerve or muscle tissue send nerve signals to an AD623 instrumentation amplifier. Two electrodes are needed since the voltage measurement is differential; therefore, one electrode serves as a reference from which voltages at the other electrode were measured. The signals then are sent through a band-pass filtering stage in order to isolate the frequencies of interest. Finally, an audio amplification stage is used in order to generate an output signal through either a speaker or a 3.5 mm audio cable, which can be used to read the signals into a computer program. An audio program called Audacity was used to record the voltage signals from the frog nerve using the audio cable, which was connected to the microphone port of a laptop computer.

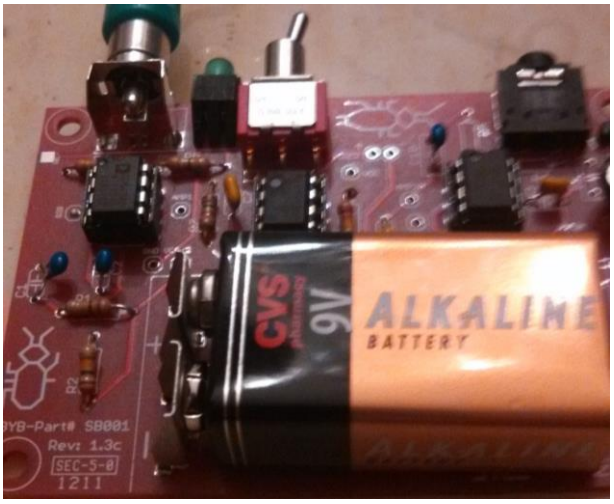

Figure 11. The SpikerBox device.

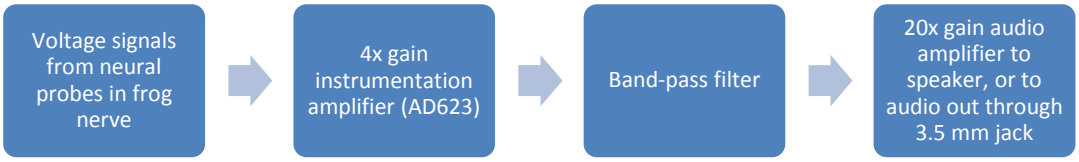

Figure 12. Flowchart of how the SpikerBox operates.

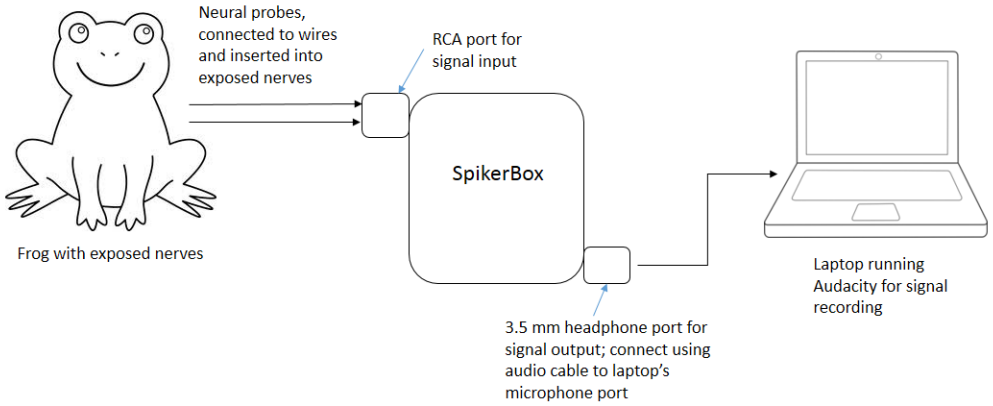

Figure 13. A diagram of the SpikerBox experimental setup.

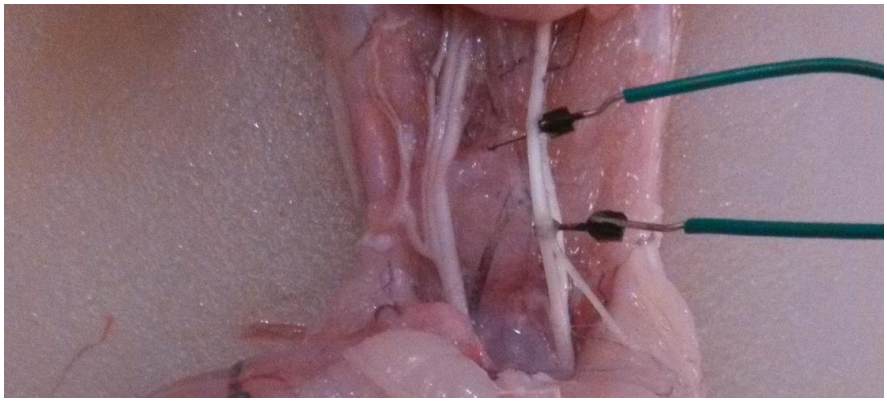

Figure 14. Neural probes connected to the SpikerBox and placed in contact with exposed frog nerves.

Nerves were not extracted from the frog for experiments using the SpikerBox. Instead, the neural probes were placed underneath an exposed nerve in the frog for recording. The probes were placed approximately 1 to 1.5 cm apart for the tests. Unlike previous tests, a stimulus voltage was not provided using a function generator. Instead, frog muscles near the nerve were physically manipulated, causing them to twitch for a period of several seconds, in order to elicit voltage signals that could be detected using the electrodes. The presence of two probes was needed to provide an appropriate input to the SpikerBox device, which relied on differential voltage measurement. During the period of muscle twitching, voltage signals from the nerve were recorded using the Audacity audio recording program.

Results

I. COMSOL simulation results

An initial simulation was conducted using a needle length of 3 mm and a load of 40 mN applied to the side and top of the neural probe needle. In the initial simulation, application of this bending force to the side of the needle shank caused deflection of the needle, with maximum stress produced near the needle tip; increasing the length of the needle increased the value of the maximum stress as well.

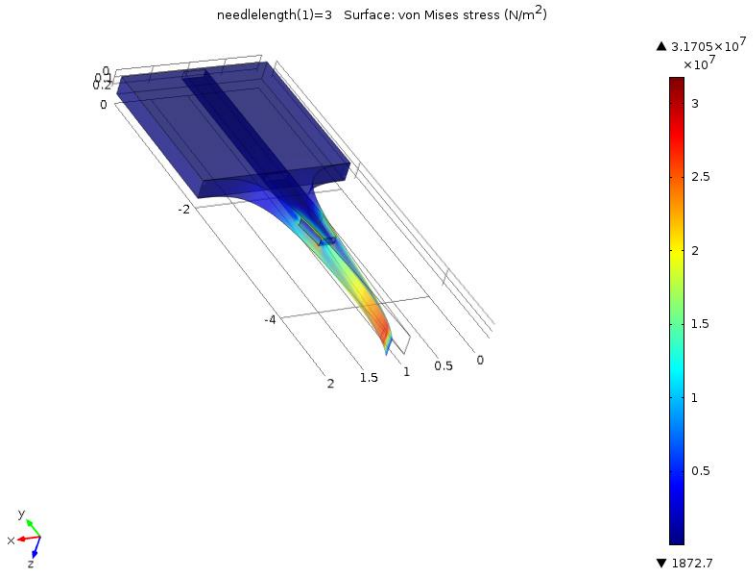

Figure 15. Output image from initial simulation after applying a 40 mN load to the side of a neural probe with a 3 mm needle. Maximum stress was produced near the needle tip.

Applying bending force to the side of the needle also appeared to produce relatively significant stress around the side ports of the fluid channel. This suggests that these side ports would also be areas of weakness, particularly if a shorter needle length was chosen. Based on the initial 3 mm simulation results, in the case of electrode needles longer than 3 mm, the tip of the needle is more likely to break. Additionally, a needle any shorter than 3 mm would not be able to penetrate the nerve to a significant depth, making it impractical for use. Increasing the needle

length past 3 mm in other simulations appeared to reduce the stress around the side ports, making a structural failure around that area less of a concern for longer needles. There was an expected deflection of the needle in the direction of the applied force, as seen in the example for a needle length of 3 millimeters. For this case, an area of higher stress is also created around the side ports of the fluid channel, and similar results were also obtained for other needle lengths longer than 3 millimeters. This suggests that the area around the fluid channel and its side ports would be another area of weakness if sufficient force were exerted on the electrode.

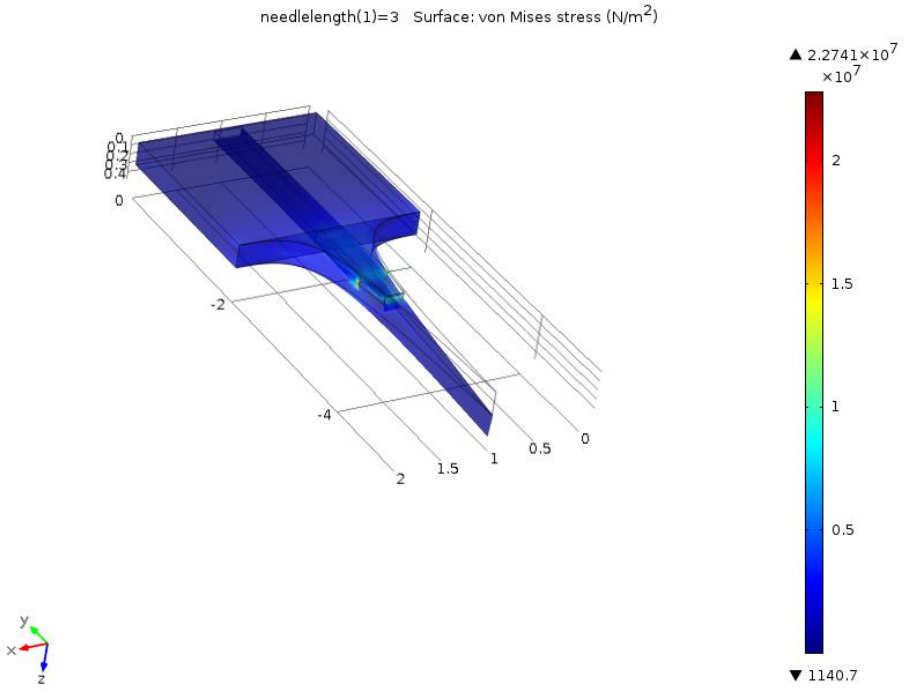

Figure 16. Output image from initial simulation after applying a 40 mN load to the top of a neural probe with a 3 mm long needle. There appears to be an area of higher stress around the exit ports of the fluid channel (red color).

Next, a larger set of simulations was conducted in order to further evaluate the application of a bending force to the top and side of the neural probe needle. Simulated loads ranging from 10 to 50 mN were applied to the left side and the top of the needle shank. The force values were chosen based on prior studies of porcine peripheral nerves, in which it was found that forces between 0.3 and 25 mN were needed to penetrate the nerves (Jensen).

The three parameters that were varied in the simulations were the length of the neural probe needle, the thickness of the neural probe, and the depth of the fluid channel below the surface. The simulations were performed for different needle lengths ranging from 3.5 to 6 millimeters, different neural probe thicknesses ranging from 0.25 to 0.5 mm, and different fluid channel distances from the surface, ranging from 35 to 85 μm.

After running the simulations, the maximum stress value for each simulation was recorded and the data were plotted in Excel in order to compare the effects of altering each variable (needle length, neural probe thickness and depth of the fluid channel from the surface). Data were plotted with different variables kept constant in order to examine the effects of each variable.

1. Effect of changing the fluid channel placement

1a. Force applied to the top of the neural probe needle

In the first set of plots, the length of the needle and the thickness of the neural probe were kept constant, and the depth of the fluid channel from the surface was varied from 35 to 85 μm. The following plots are all from simulations using an applied force of 10 mN to the top of the neural probe.

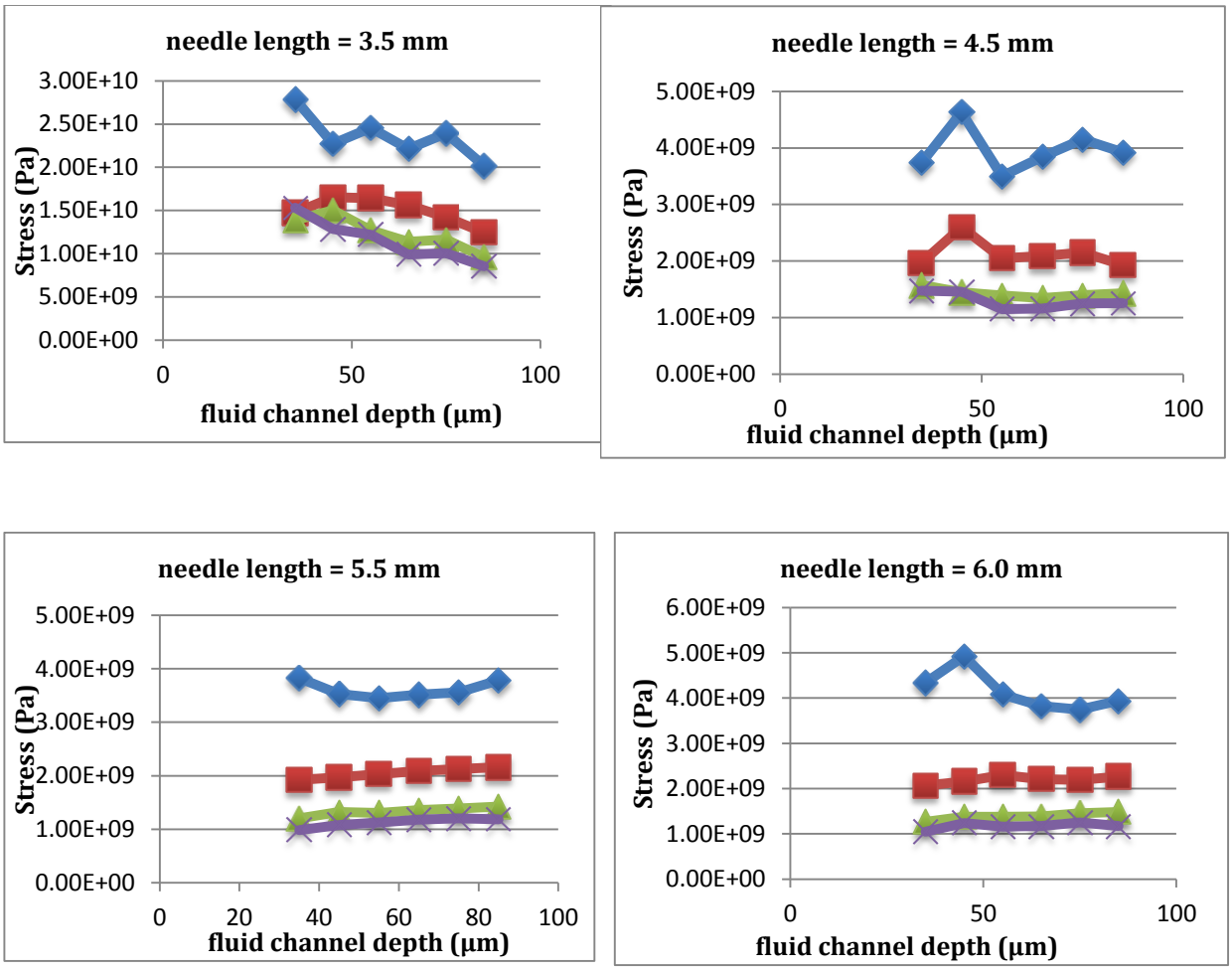

Figure 17. Plots of maximum stress in the neural probe versus the depth of the fluid channel, for neural probe thicknesses from 0.25 to 0.5 mm. The force was applied to the top of the neural probe needle in the simulations.

The top left plot shows the results for a needle length of 3.5 mm. Each set of points in the plot represents a different neural probe thickness. From the plot, it can first be seen that increasing the depth at which the fluid channel is placed will reduce the maximum stress seen by the electrode. Additionally, it also appears that increasing the neural probe thickness will decrease the maximum stress by approximately a factor of 2 when comparing a thickness of 0.25

mm to 0.5 mm. However, the difference in stress values between thicknesses of 0.45 mm and 0.5 mm is not nearly as great.

After increasing the needle length to 4.5 mm, the maximum stresses appear to have decreased by an order of magnitude compared to the 3.5 mm long needle. Like in the previous plot, the 0.25 mm thick neural probe feels the highest value of stress compared to thicker probes. As the thickness is increased, the maximum stress decreases. However, unlike the previous plot, changing the depth of the fluid channel did not appear to have as significant of an effect on stress values.

When increasing the needle length to 5.5 mm, the maximum stresses appear to be in a similar range to the stresses for the 4.5 mm needle, with the thickest neural probe again experiencing the lowest amount of stress. Increasing the needle length further to 6.0 mm also gives maximum stresses within approximately the same ranges as the 4.5 and 5.5 mm long needles. The maximum stress values stay fairly stable across different channel depths for neural probe thicknesses above 0.35 mm.

Based on the results after applying a force of 10 mN, changing the depth at which the fluid channel is placed below the surface of the neural probe does not appear to significantly influence the maximum amount of stress felt by the probe, except at a needle length of 3.5 mm. Neural probe thickness had the greatest effect on the maximum stress level, but since the 0.45 and 0.5 mm thick neural probes had very similar values, this effect may not be as great as the thickness continues to increase.

1b. Force applied to the side of the neural probe needle

In this set of simulations, a force of 10 mN was applied to the side of the neural probe needle. The plots compare simulation data that have identical probe thicknesses and needle lengths while varying the channel depth.

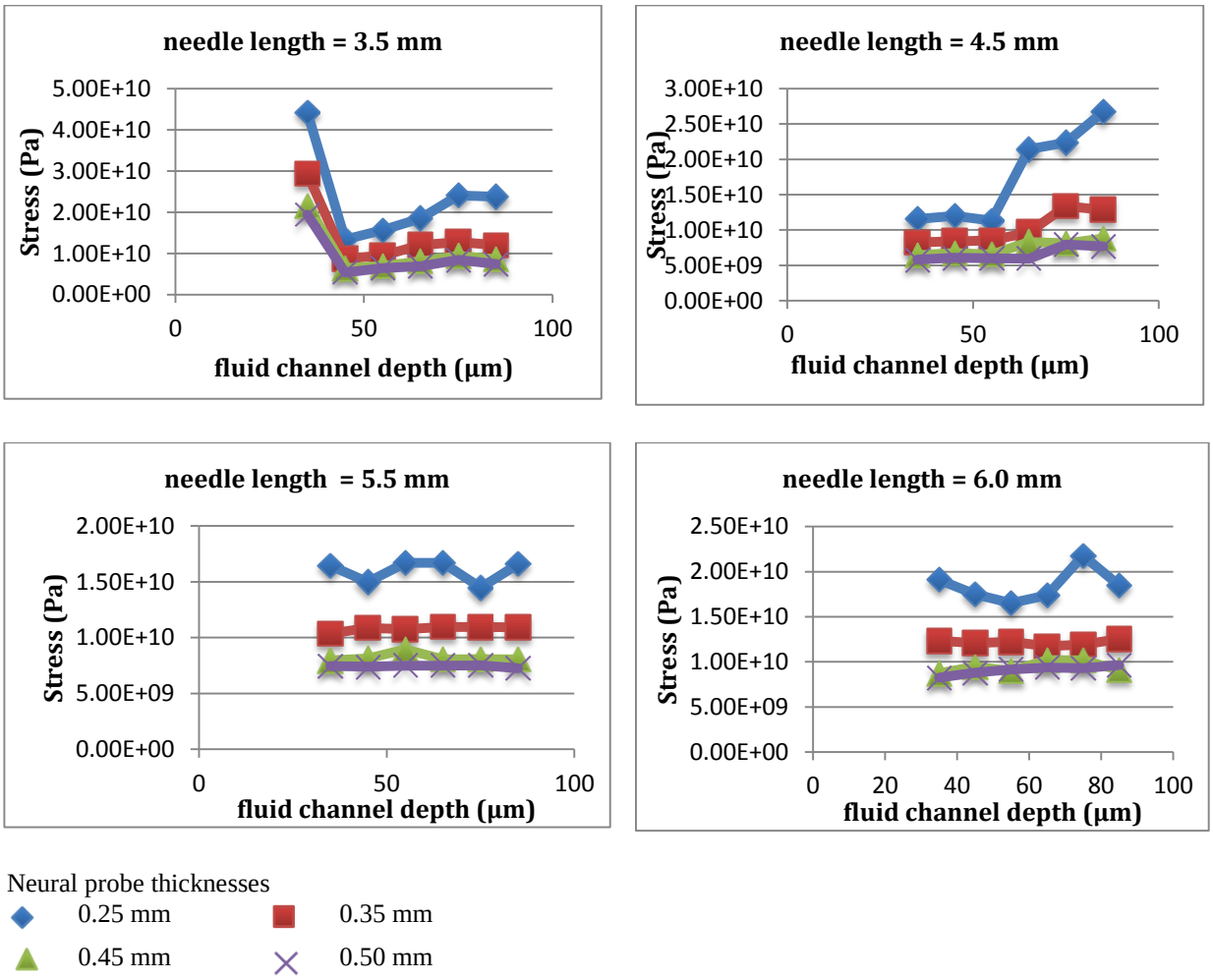

Figure 18. Plots of maximum stress versus fluid channel placement for neural probe thicknesses from 0.25 to 0.5 mm. The force was applied to the side of the neural probe needle in the simulations.

For a needle thickness of 3.5 mm, there is an unusual spike in the maximum stress at a channel depth of 35 µm. The stress drops down to a lower value for channel depths of 45 µm, and there is then a steady increase in maximum stress value as the channel is placed deeper below the surface of the neural probe. There is a large difference in stress between the 0.25 mm

thick probe and the other probe thicknesses, and the 0.45 mm and 0.5 mm thick neural probes appear to have very similar values for maximum stress.

When the length is increased to 4.5 mm, all of the probe thicknesses have similar maximum stress values initially from channel depths of 35 to 55 μm. Starting at a depth of 65 μm, the stress appears to increase, with the stress values for the 0.25 mm thick probe more than doubling. As the length of the needle is further increased to 5.5 mm, the effect of changing the channel depth becomes less pronounced. For neural probe thicknesses of 0.35 mm and above, the stress values remain very similar as the channel depth is increased. Increasing the needle length to 6 mm shows that while a neural probe thickness of 0.25 mm appears to have a significant amount of variation in maximum stress values as the channel depth is increased, thicknesses 0.35 mm and above are much more stable.

Based on the plots, for thicknesses greater than 0.25 mm and needle lengths greater than 4.5 mm, changing the depth at which the fluid channel is placed does not appear to significantly affect the maximum stress felt by the probe. The depth of the fluid channel may not be a significant consideration for the design of the probe.

2. Effect of changing neural probe thickness

2a. Force applied to the top of the neural probe needle

As in the previous section, the following plots are from the set of simulations where the applied force was 10 mN. In these plots, the fluid channel depth and needle length are kept the same, while the thickness of the neural probe is varied from 0.25 to 0.5 mm.

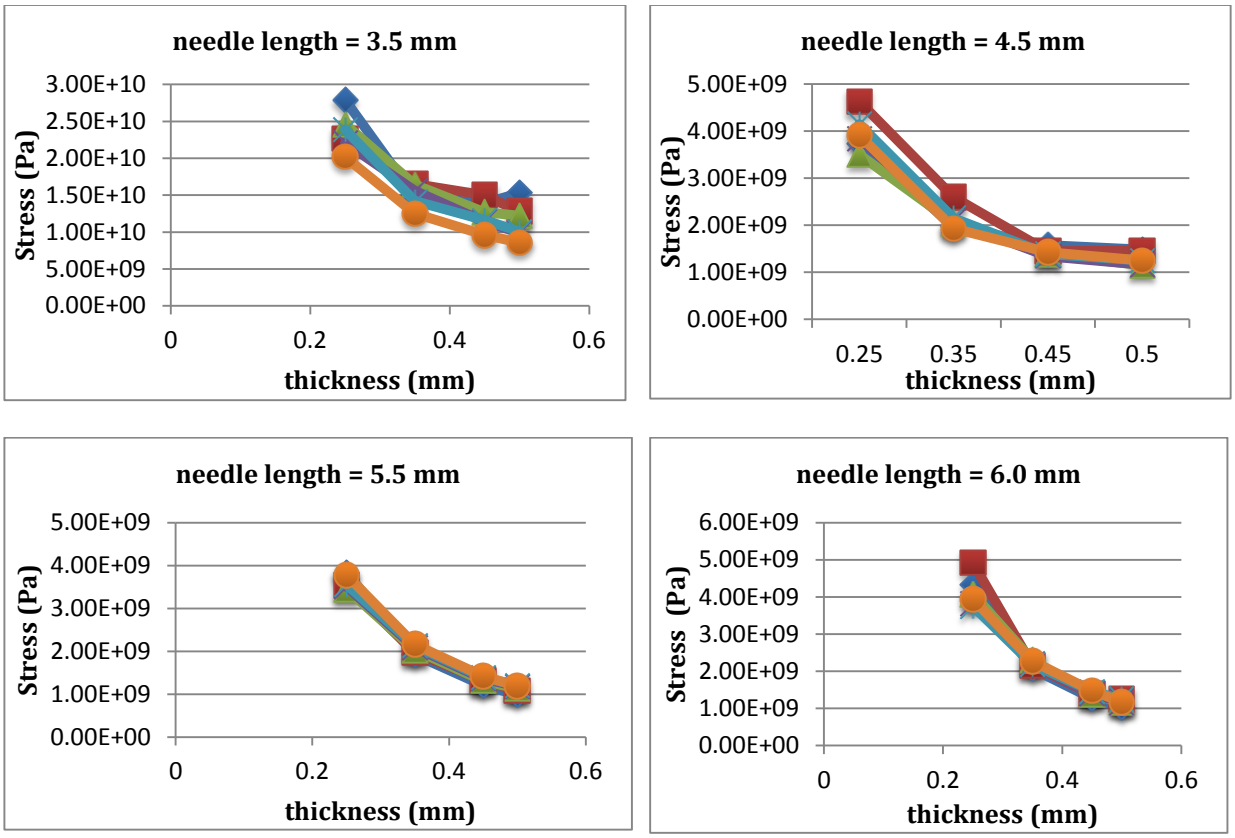

Figure 19. Plots of maximum stress versus thickness when keeping fluid channel depth constant; needle lengths were from 3.5 to 6 mm. Force was applied to the top of the neural probe needle for these simulations.

For a neural probe with a needle length of 3.5 mm, there is a clear decrease in the maximum stress as the thickness of the neural probe increases. There is a sharp decrease from 0.25 to 0.35 mm, but the stress level appears to reach a plateau after 0.5 mm. Additionally, the maximum stress decreases as the fluid channel is placed deeper below the surface of the probe. Although this is true for a needle length of 3.5 mm, this trend may not continue for longer needle lengths.

When the needle length is increased to 4.5 mm, the same general trend can be seen as in the previous plot where the needle length was 3.5 mm, in which the maximum stress decreases as the probe thickness is increased. Maximum stress values for all neural probe thicknesses have also decreased when compared to the previous plot. However, unlike the previous plot, in which the different channel depths had a small but noticeable effect on the maximum stresses, there does not appear to be a similar effect here. For needle lengths 4.5 mm and greater, the channel depth may not be a significant factor.

When increasing the needle length to 5.5 mm, the plot again shows that increasing the thickness will decrease the maximum stress. Interestingly, the stress values are clustered more closely together in the plot compared to previous plots, further supporting the assertion that the channel depth is not a particularly significant factor compared to thickness. The maximum stress values themselves are similar to the previous needle length.

After the needle length was increased to 6 mm, the same general trend can be observed in which increasing thickness decreases maximum stress. There is greater variation in the maximum stress values for the lower thickness of 0.25 mm compared to the other thickness values. Increasing the thickness beyond 0.35 mm may negate the effect of changing the channel depth, as channel depth does not appear to make a significant difference to the maximum stress.

2b. Force applied to the side of the neural probe needle

In this set of simulations, a force of 10 mN was applied to the side of the neural probe needle. In the plots, all data points with the same needle length are compared while the channel depth is varied.

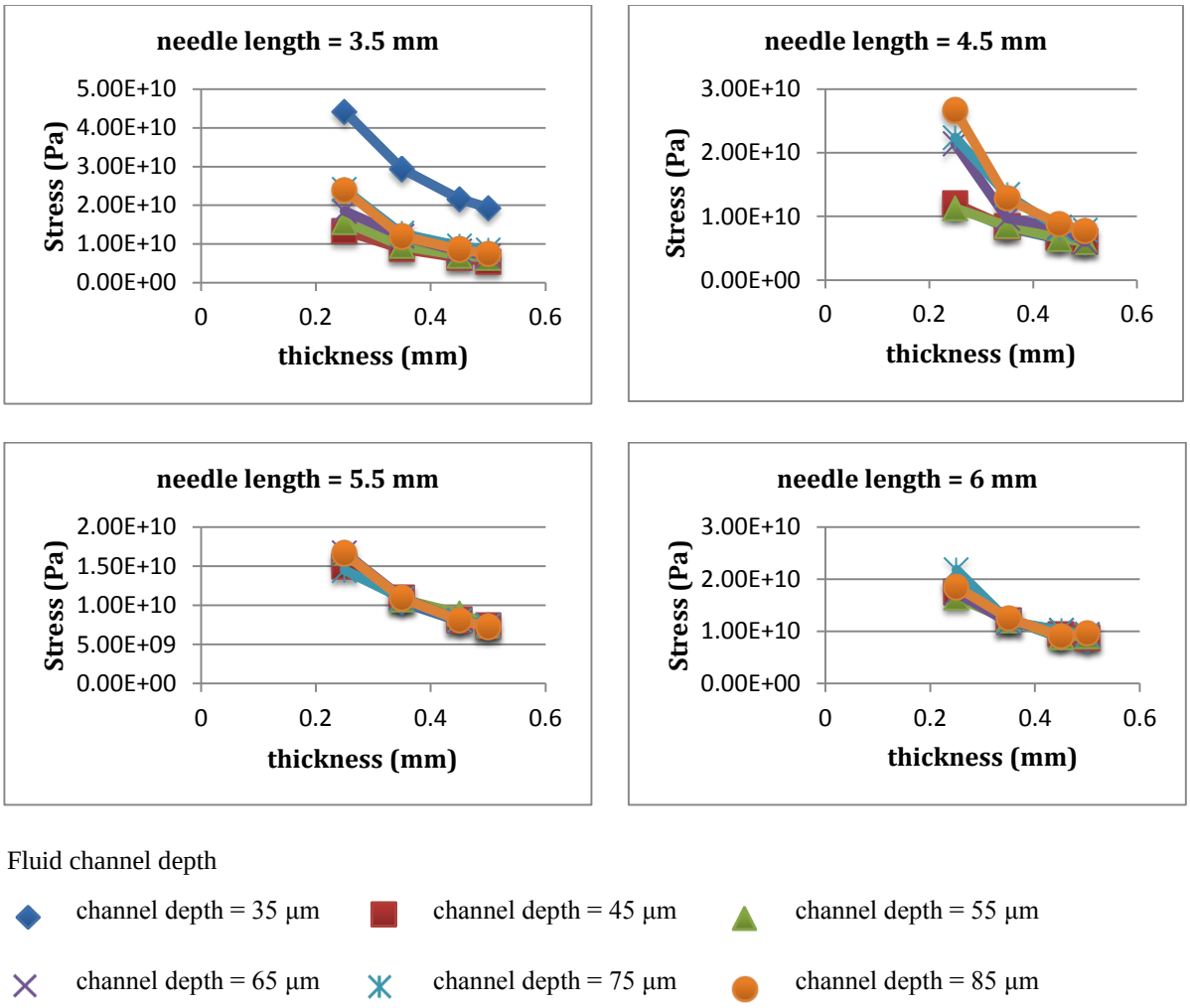

Figure 20. Plots of maximum stress versus thickness when keeping fluid channel depth constant, for needle lengths between 3.5 and 6 mm. Force was applied to the side of the neural probe needle for these simulations.

For a needle length of 3.5 mm, there is a downward trend in maximum stress with increasing thickness. Interestingly, there is a large difference between maximum stress values between a channel depth of 35 and a channel depth of 85. As the channel depth increases, this difference becomes less significant. The difference is most pronounced at a thickness of 0.25 mm.

For a needle length of 4.5 mm, it is unusual to see that the needle with channel depth 85 has the highest stress for a 0.25 mm thick needle. Other than that, the same downward trend can

be observed. While there is a large disparity in stress values for a 0.25 mm thick needle, the stresses become closer together as the thickness is increased.

The same downward trend can be seen for a needle length of 5.5 mm. Unlike the previous needle lengths, the stress values are more tightly clustered together. This suggests that the effect of channel depth becomes more and more negligible as the needle length increases. Relative to the previous plots, the maximum stress is lower, with the highest values not exceeding 1.80 x 10^{10}. Finally, for a needle length of 6 mm, we see that the maximum stress value in the plot is slightly higher than for a needle length of 5.5 mm. The same downward trend is observed here as well.

Overall, it appears that the effect of changing thickness has the most pronounced effect on maximum stress for a shorter needle length of 3.5 mm. As the needle length is increased, stress is approximately halved when doubling the neural probe thickness. The shorter needles also experience more stress regardless of thickness. The effect of changing channel depth is most pronounced for shorter needle lengths as well. As needle length is increased, channel depth becomes less and less of a factor in the maximum stress values.

3. Effect of changing neural probe needle length

3a. Force applied to top of neural probe needle

As in the previous section, a force of 10 mN was applied to the neural probe needle. The needle length was varied between 3.5 and 6 mm for the following plots. Each plot compares identical thicknesses while varying the needle lengths. Each set of points represents a different fluid channel depth.

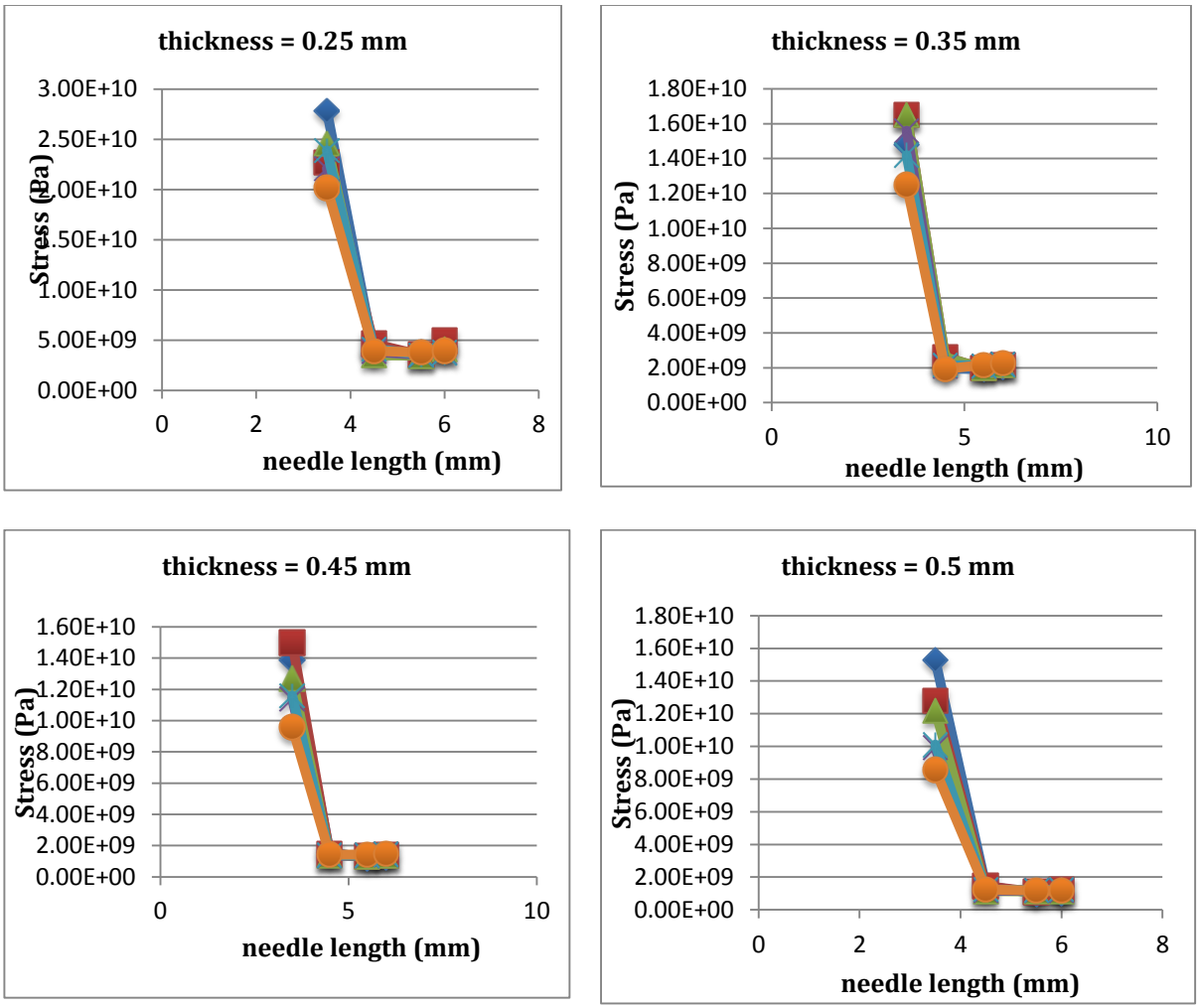

Figure 21. Plots of maximum stress versus needle length for thicknesses from 0.25 to 0.5 mm. Force was applied to the top of the neural probe needle for these simulations.

Initially, the stress value is relatively high for the 3.5 mm needle. There is some variation in the maximum stress values for a 3.5 mm needle as well. After the needle length is increased to 4.5 mm and longer, the stress values are more stable at around 5.00 x 10^9. Based on these results, it appears that the needle length may not have a significant effect on reducing stress past 4.5 mm.

The plot for a neural probe thickness of 0.35 mm appears very similar to the previous plot (neural probe thickness of 0.25), although the maximum stress values have decreased. Again, after increasing the length of the needle past 3.5 mm, the maximum stress values become more stable.

In the plot for a thickness of 0.45 mm, the stress values for a 3.5 mm needle are relatively high, but stress vales for the other needle lengths remain more consistent. The graphs appear to support the assertion that needle length does not have a significant effect past 3.5 mm. Fluid channel depth does not appear to be significant either, as the stress values are nearly identical. The stress values for both the 0.35 and 0.45 thick probes are very similar for 4.5 mm and longer needles. The 0.45 thick probes are about 1.5×10^9 while the 0.35 thick probes stay at about 2.00×10^9.

For a thickness of 0.5 mm, the plot appears to be following the same behavior as previous plots in this set. The stress values for the 3.5 mm needle are also fairly similar to the previous plots as well. The maximum stress values for the needles 4.5 mm and longer are slightly lower than the previous plots, with values of about 1.2×10^9.

Based on these results, increasing the needle length past 3.5 mm to 6 mm does not appear to affect the maximum stress significantly. Changing the neural probe thickness still appears to be the most significant factor in the maximum stress felt by the neural probe.

3b. Force applied to side of neural probe needle

For the following set of plots, a force of 10 mN was applied to the side of the neural probe needle. The plots examine the effect of changing needle length while maintaining constant thickness and channel depths. Each plot contains the data points for a specific neural probe

thickness, from 0.25 mm to 0.5 mm, while varying the fluid channel depth from 35 µm to 85 µm below the surface.

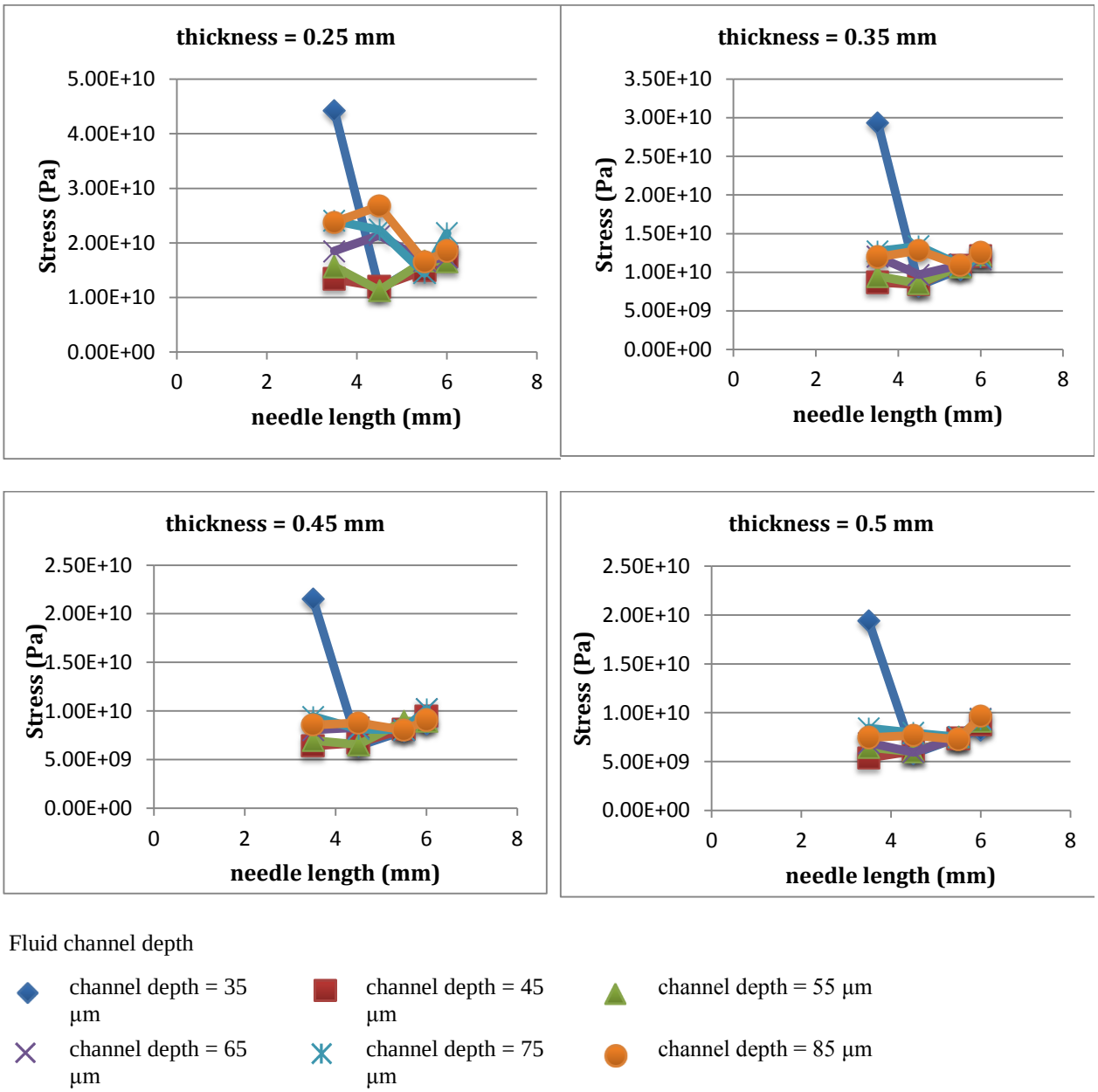

Figure 22. Plots of maximum stress versus needle length, for thicknesses between 0.25 and 0.5 mm. Force was applied to the side of the neural probe needle.

For a channel depth of 35 µm, there is an initially high stress value for the 3.5 mm long needle. The stress then drops for the 4.5 mm long needle before slowly increasing as the needle

length increases. For other channel depths, the behavior is somewhat different. For example, for the channel depth of 85 µm, the stress for a 4.5 mm needle is actually greater than that of a 3.5 mm needle.

When the thickness is increased to 0.35 mm, the maximum stress values decrease compared to the 0.25 mm thick neural probes. With the exception of the stress value for the 3.5 mm probe with 35 µm channel depth, the stress values appear to be more stable as well, with all of the values staying below 1.30×10^{10} and above 8.0×10^{9}. It seems that having the needle length at 4.5 mm and higher and the probe thickness at 0.35 mm or higher will produce more similar stress values when a force is applied to the side of the needle.

As the thickness is increased to 0.45 mm, the stress for the 3.5 mm needle still stays unusually high at the 35 µm channel depth. However, like the previous plot, the stress values are more stable compared to the 0.25 mm thickness plot. The maximum stress values decrease as well relative to the previous plots, so increasing thickness does have a noticeable effect on reducing stress. When comparing relatively shallow and deep channel depths, such as 45 µm and 85 µm, the increased channel depth does appear to make the stress values more stable as well. At 45 µm, there is a slight increase in the stress values as needle length is increased, while at 85 µm, the stress values stay closer to each other. However, as the stress values are higher for the 85 µm depth, there is not any advantage to selecting that particular channel depth.

Finally, when thickness is increased to 0.5 mm, the stress values do not decrease by very much compared to the previous plot for the 0.45 mm thickness. Increasing the thickness past 0.45 mm may not have a significant effect on reducing the stress. Again, the 3.5 mm needle and 35 µm channel depth combination has an unusually high stress compared to the other probes.

The lowest stress appears to be for the combination of 3.5 mm needle length and 45 μm channel depth, with a value of 5.37×10^9.

For the purposes of minimizing stress when applying force to the side of the neural probe, a length of 4.5 mm or longer appears to be beneficial, although the stress does generally increase somewhat as the needle length is increased. A longer needle length will also make the neural probe more useful, as it will be able to contact more axons when embedded within a nerve fiber. It appears that increasing the needle length too far will increase the chance of breakage when force is applied to the side of the needle, so limiting this parameter is necessary.

4. COMSOL simulation summary

Based on the simulation results, the most significant factor influencing the amount of stress felt by the neural probe under an applied load is the thickness of the neural probe. Increasing the thickness of the probe reduces the amount of stress that it experiences under the same load. However, increasing the thickness past 0.45 mm may not reduce the stress significantly, so there may be an optimum value for thickness between 0.25 mm and 0.5 mm that will optimally reduce stress. The depth of placement of the fluid channel below the probe's surface did not appear to have a significant effect on the maximum stress. The length of the neural probe needle also did not appear to affect stress significantly when the needle was 4.5 mm or greater in length.

Overall, the thickness of the neural probe should be from 0.35 mm to 0.5 mm, as the effects of increasing thickness beyond 0.5 mm on maximum stress are not very significant. There is a noticeable benefit to making the thickness greater than 0.25 mm. A 3.5 mm needle does not appear to be practical and also suffers from the greatest amount of stress. An increase in the needle length to 4.5 mm or longer appears to work well in minimizing the stress. A length of 5.5

mm may be ideal in keeping the stress low, as making it greater than 6 mm caused the stress values to increase. Since the depth of placement of the fluid channel did not have a significant impact, the placement is not particularly important when considering the design of the neural probe.

II. Electrical testing results

1a. Initial electrical test using saline solution

The ability of the neural probe to conduct electrical signals was verified using LabVIEW and the myDAQ data acquisition tool. Two neural probes connected to the input and output ports of the myDAQ were placed in a conductive 0.9% saline solution at room temperature. A sinusoidal signal created using the function generator in LabVIEW and sent through the neural probe connected to the analog output of the myDAQ was successfully detected through the neural probe connected to the myDAQ's analog input. As seen in the following figure of the program output, the results of the initial test demonstrated that the neural probes were able to transmit and receive the sine wave signal through the saline solution. The function generator provided in LabVIEW was also able to produce other types of functions, such as square and sawtooth functions, which were tested with similar results.

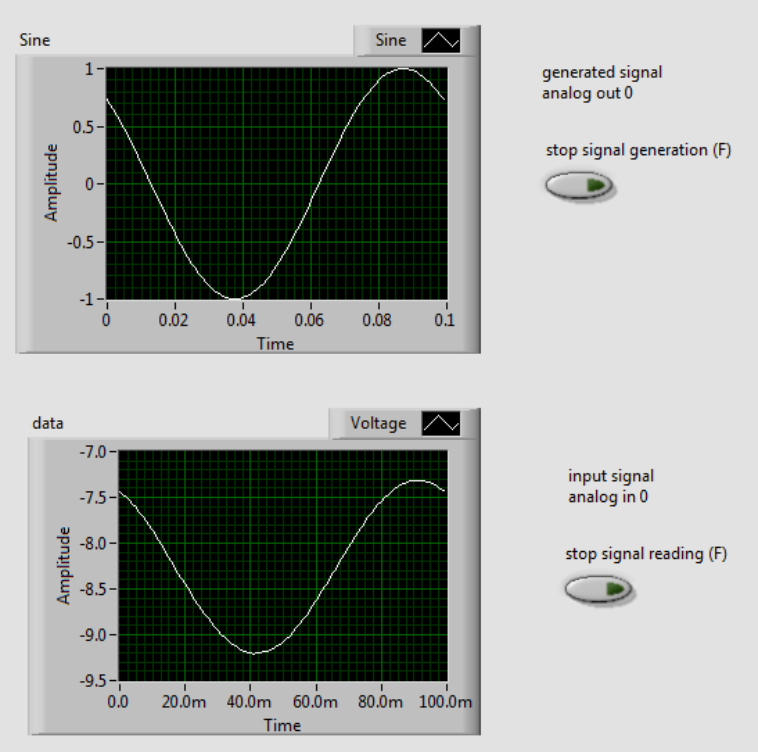

Figure 23. Sample output of the program after inserting both probes into the saline solution. The top graph shows the generated signal, while the bottom graph shows the signal received by the neural probes.

1b. Initial electrical test in frog tissue

The electrodes were also directly inserted into an exposed nerve of the frog, while using the same LabVIEW program to test electrical conductivity. The results of this test were very similar to the first test using the small petri dish of 0.9% saline solution. It was found that simply touching the neural probes on any point on the body of the frog would result in identical signals being displayed for both the input and the output of the LabVIEW program. This was because the entire body of the frog acted as a conductor that was able to transmit the signal back into the input probe. Additionally, there were no input signals that resembled nerve action potentials, which was the desired result; this suggested that a better approach was needed in order to produce meaningful results.

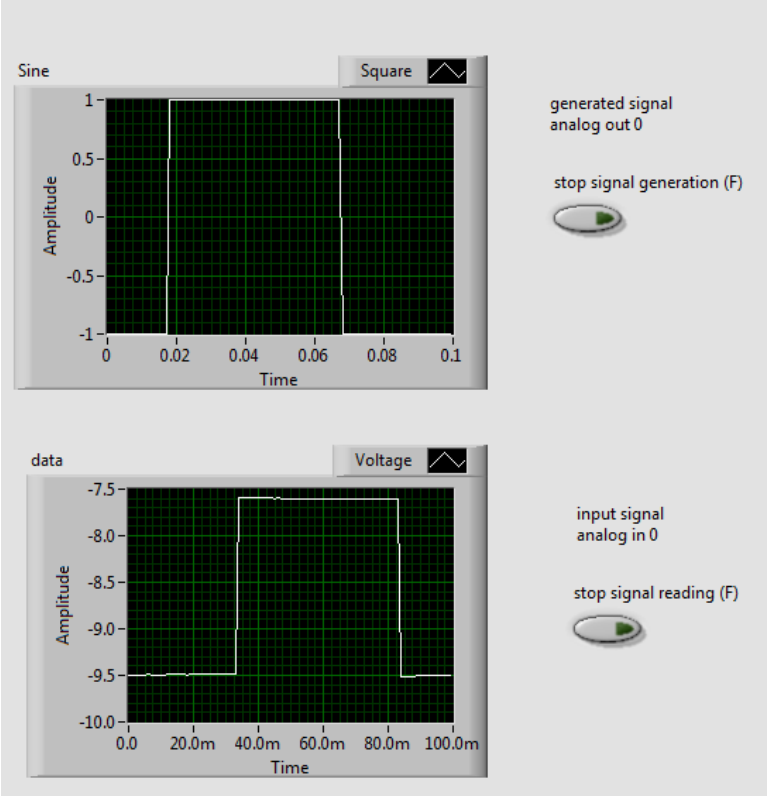

Figure 24. A sample result of the first test using frog nerve. The same signal shape was seen for both input and output, with a slight delay in the analog input.

2. Frog sciatic nerve experiment

Unfortunately, the frog sciatic nerve experiment using LabVIEW did not demonstrate useful results, both when the nerve was left in the body of the frog and when the nerve was removed from the frog and laid over the two neural probes. Many of the attempts to record signals using the LabVIEW software showed a significant amount of noise and were difficult to recognize. Another approach to recording the voltage signals was needed in order to demonstrate that the neural probes could function with biological tissue, so the SpikerBox device was used for further experiments. For experiments where the nerve was removed from the body, the length of time for which the sciatic nerves were exposed to air, as well as the method used to extract the

nerves from the frog leg, may have caused damage that made the nerves non-viable for the experiment.

3. Recording nerve signals using the SpikerBox

Using the SpikerBox neurophysiology device with the neural probes showed better results from recording compared to the previous approaches using LabVIEW. The neural probes were able to successfully record sequences of rapidly firing action potentials in exposed frog nerve, which were caused by mechanical stimulation of the frog muscles near the nerve. The process of stimulation and recording was repeated several times, with similar results each time, until the frog was no longer viable. During the period of stimulation, in which the frog's muscles were observed to rapidly twitch, a characteristic pattern in the signal emerged occurring in rapid succession, which was suggestive of action potentials being propagated along the nerve, as seen in the figure. As the nerves were made up of a bundle of nerve fibers with varying characteristics, the recorded signals represented the sum of the responses of all of the nerve fibers. The recordings also show a characteristic shape of action potentials, in which there is a depolarization to a threshold voltage, followed by a sharp depolarization or "spike," after which a period of repolarization to the baseline voltage occurs. The shape of the recorded signals appeared to change between recording sessions, which was likely due to movement of the neural probes along the nerve. Additionally, the amplitude of the signals decreased over time until the nerves were no longer viable and able to produce signals.

The following plots recorded in the Audacity audio program display the recorded nerve signal waveforms, with time given in seconds and milliseconds on the x-axis and a normalized amplitude measurement from -1 to +1 on the y-axis. Audacity did not have an option to display

the waveform using absolute voltage measurements. The amplitudes ranged from a minimum of -1 to a maximum of approximately 0.6 on the normalized scale.

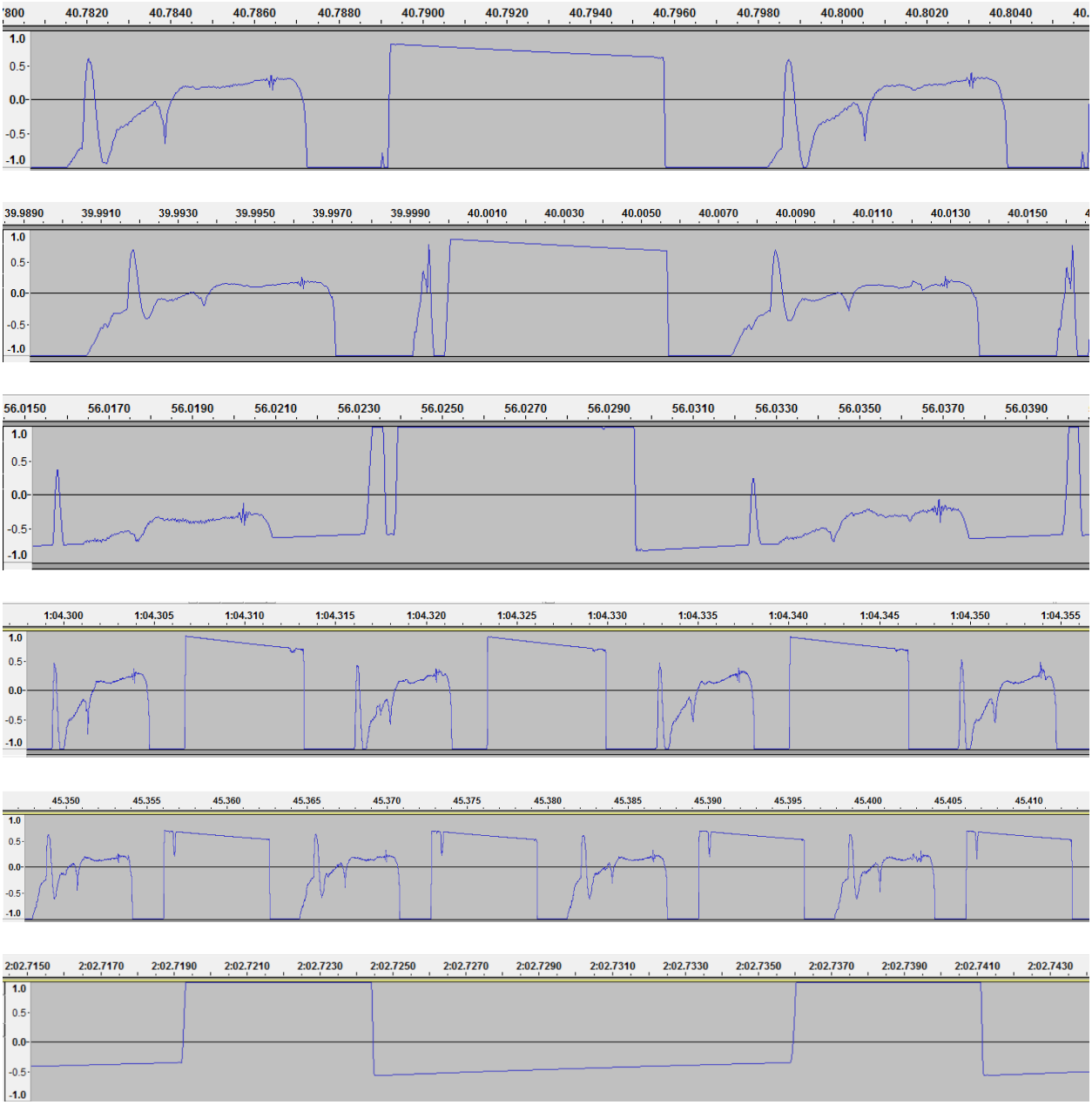

Figure 25. Example recordings of voltage signals from the neural probes using the SpikerBox, with time on the x-axis in seconds and milliseconds, and a normalized amplitude scale from -1.0 to +1.0 on the y-axis. Each of the recordings were taken from different sessions of muscle stimulation. For comparison, the last recording shows a period where no stimulation was taking place.

The results of the experiment using the SpikerBox demonstrated that the neural probes were capable of interfacing with biological tissue and recording signals from nerve tissue.

Conclusion

A 3D model of the neural probe design was created using SolidWorks software. Initially, the model was imported directly into COMSOL, but this approach made it difficult to dynamically change model parameters, which was necessary for the simulation. A new 3D model matching the original SolidWorks model was created using COMSOL. The structural mechanics module of COMSOL was used to perform simulations in which a load from 10 to 50 mN was applied to the top and the side of the model. During the simulation, several parameters of the model were set as variables so that they could be modified. These variables were the length of the needle, depth of the fluid channel, and thickness of the neural probe. The simulation ran through each combination of parameters in order to produce an image of the stresses on the neural probe under the applied load. The stresses on the simulated model were then examined in order to determine which parameters had an effect on the stresses and what values or ranges of values could optimally be used for those parameters.

From the simulation results, it was found that having the thickness of the needle be about 0.35 mm to 0.5 mm would be appropriate, as increasing the thickness past 0.5 mm did not have a significant impact on stress reduction. Additionally, a needle that is too thick would prove to be impractical for implantation, as it would potentially cause too much damage to the nerve. The placement of the fluid channel did not appear to make a significant impact on the stress, so this factor can be varied without much effect. Finally, a needle length of at least 4.5 mm but less than 6 mm appears to be ideal, as it would be able to contact a larger number of axons than a shorter needle while also having lower stress under the same load.

Based on the results of electrical testing, the neural probes were able to conduct and receive signals through a conductive saline solution, and can also record signals from biological

tissue, specifically frog nerve. The design of the devices includes multiple conductive wires that are intended to stimulate and receive multiple signals from individual nerve axons for finer control, but this capability was not tested. However, recording of a compound action potential signal from a nerve was demonstrated to be possible.

References

Grill, Warren M., Sharon E. Norman, and Ravi V. Bellamkonda. "Implanted neural interfaces: biochallenges and engineered solutions." *Annual Review of Biomedical Engineering* 11 (2009): 1-24.

Rutten, Wim LC. "Selective electrical interfaces with the nervous system." *Annual Review of Biomedical Engineering* 4.1 (2002): 407-452.

Ziegler-Graham, Kathryn, et al. "Estimating the prevalence of limb loss in the United States: 2005 to 2050." *Archives of physical medicine and rehabilitation*89.3 (2008): 422-429.

Raichle, Katherine A., et al. "Prosthesis use in persons with lower-and upper-limb amputation." *Journal of rehabilitation research and development* 45.7 (2008): 961.

Stewart, JD." Peripheral nerve fascicles: anatomy and clinical relevance." *Muscle Nerve*. 28 (2003) 525– 41.

Branner, Almut, et al. "Long-term stimulation and recording with a penetrating microelectrode array in cat sciatic nerve." *Biomedical Engineering, IEEE Transactions on* 51.1 (2004): 146-157.

Sergi, Pier Nicola, et al. "Biomechanical characterization of needle piercing into peripheral nervous tissue." *Biomedical Engineering, IEEE Transactions on* 53.11 (2006): 2373-2386.

Jensen, Winnie, et al. "Measurement of intrafascicular insertion force of a tungsten needle into peripheral nerve." *Engineering in Medicine and Biology Society, 2001. Proceedings of the 23rd Annual International Conference of the IEEE*. Vol. 3. IEEE, 2001.

Fernández, Luis J., et al. "Study of functional viability of SU-8-based microneedles for neural applications." *Journal of Micromechanics and Microengineering* 19.2 (2009): 025007.

Nicholson, Kristen J., and Beth A. Winkelstein. "Nerve and Nerve Root Biomechanics." *Neural Tissue Biomechanics*. Springer Berlin Heidelberg, 2011. 203-229.

Tijero, M., et al. "SU-8 microprobe with microelectrodes for monitoring electrical impedance in living tissues." *Biosensors and Bioelectronics* 24.8 (2009): 2410-2416.

Olansen, J. B., et al. "Using virtual instrumentation to develop a modern biomedical engineering laboratory." Int. J. Eng. Educ. 2000.

Biomedical Systems and Instrumentation Group. "Electroneurology". Rice University. Houston, TX.